

residual ash is enriched in silica and applied as a good adsorbent material for heavy metals [2].

The capture of carbon dioxide and other smoke gases from the biomass burning can be vitally achieved through hot manganese oxide at 200-250°C. The gases change the mineralogical composition of the applied manganese oxides ore as investigated by using XRD, IR and SEM-EDX analysis. The environmental impact of the process can be deduced from the significant change in the mineralogy of the manganese ore from mainly oxide forms to carbonate and halide rich phases. The ore impurities (e.g. Na, Mg, Ca, Al and F) contribute largely in the obtained mineral phases.

[1] Turn, S. Q., Jenkins, B.M., Chow, J.C., Pritchett, L.C., Cahill, T. and Whalen, S.A., *J. Geophysical Research*, 1997, 102 (D3), 3683-3699. [2] Bishay, A. F., *AJEST* (Accepted 2010, Under publication).

Keywords: CO₂-sequestration, biomass burning, manganese mineralogy.

FA2-MS16-P22

Saccharide Yield From Interacted Biomass With Oxide Minerals For Separation and Fractional Crystallization In Acidic Route Of Mineral Processing. A.F. Bishay. *Nuclear Materials Authority, Cairo, Egypt*.

E-mail: abram_bishay2002@yahoo.com

Voluminous bio-wastes are resulted every year from agriculture where extensive literature review the article of their acidic dissolution [1]. The presence of organic matter represent a triggering factor that controls mineral dissolution in the acid sulfate soil [2]. For implications, rice straw is very promising material in the sulfate medium of mineral processing. The dissociated biomass promotes dissolution, separation and crystallization of oxide minerals avoiding the extra cost.

Under controlled boundary conditions and at room temperature, rice straw in dilute sulfate medium using sulfuric acid and manganese oxide yield saccharides and manganese sulfate crystals. Moreover, under drastic acidic conditions and biomass subjection into ilmenite sulfate process, reduced saccharide is obtained with the facility of continuous crystallization of iron sulfate off. The end-product is a cheap and chemically controlled nano-TiO₂ which find many photocatalysis applications.

[1] Li, C., Knierim, B., Manisseri, C., Arora, R., Scheller, H.V., Auer, M., Vogel, K. P., Simmons, B.A. and Singh, S., *Bioresource Technology*, 101 (13), 2010, 4900-4906.

[2] Chengxing, C., Chuxia, L., Yonggui, W., Wenzhou, L., Jie, L., *Australian Journal of Soil Research*, 2006, 3840.

Keywords: Biomass, mineal processing, saccharides.

FA2-MS16-P23

Al/Si-ordering phenomena in sanidine megacrystals from the Eifel. Kathrin Demtröder, Sara Dehn, Michael Gopon, Jürgen Schreuer. *Institut für Geologie, Mineralogie und Geophysik, Ruhr-Universität Bochum, Germany*.

E-mail: schreuer@rub.de

Sanidine megacrystals from Volkesfeld (Rieden eruptive centre, East Eifel volcanic field, Germany) are well known for their unusual optical properties [1]. Starting from 1025 K their optic axial angle $2V$ changes rapidly at higher temperatures. This macroscopic effect has been interpreted as being associated with a corresponding increase of the Al/Si-disorder on the atomic level. The sanidines from Volkesfeld are further characterised by very low concentrations of dislocations indicating hydrothermal growth conditions [3]. However, the reason for the drastic and irreversible change of the optical properties is still under debate.

To clarify the role of water and chemical composition for the observed optical anomalies, the Al/Si-ordering has been investigated in sanidine megacrystals from four different eruptive centres of the Eifel and from Madagascar (served as reference) by means of single crystal X-ray diffraction, optical techniques and NMR-spectroscopic studies.

The chemical composition Na_xK_{1-x}AlSi₃O₈, as obtained by electron microprobe analysis, is characterised by $x \approx 0.15$ and $x \approx 0.27$ for megacrystals from the East Eifel and West Eifel volcanic field, respectively, with up to 2 at-% celsian and less than 0.02 at-% anorthite. The H₂O content varies between about 250 ppm and 400 ppm.

All investigated Eifel sanidines show irreversible optical anomalies at temperatures above 1073 K. Their optical axis angles $2V$ change drastically from about 30° in a plane perpendicular to (010) to about 35° within (010). According to [2] this corresponds to a decrease in the Al/Si order from $2t_1 \approx 0.70$ to 0.58. However, tetrahedral bond distances derived from single crystal structure analyses indicate $2t_1 \approx 0.58$ [4] for fresh samples and only small changes after annealing. The latter findings are supported by ²⁹Si and ²⁷Al NMR-experiments. Our contradictory experimental observations are probably caused by the water dissolved in the crystal structure of these nominally anhydrous minerals.

[1] C. Zeipert, W. Wondratschek: Ein ungewöhnliches Temperverhalten bei Sanidinen von Volkesfeld/Eifel. *N.Jb. Mineral., Mh.* 9 (1981) 407-415. [2] S.-C. Su, P.H. Ribbe, F.D. Bloss: Alkali feldspars: Structural state determined from composition and optic axial angle $2V$. *Am. Min.* 71 (1986) 1285-1296. [3] W. Widder, H. Wondratschek, M. Fehlmann, H. Klapper: X-ray topographic study of Eifel sanidine (Volkesfeld). *Z. Kristallogr.* 209 (1994) 206-209. [4] P.H. Ribbe, G.V. Gibbs: Statistical analysis and discussion of mean Al/Si-O bond distances and the aluminum content of tetrahedra in feldspars. *A. Min.* 54 (1969) 85-94. [5] Su, S. C., Bloss F. D. & Ribbe P. H. (1984): Optical axial angle, a precise measure of Al, Si ordering in T 1 tetrahedral sites of K-rich alkali feldspars. - *Am. Min.* Vol. 69: 440-448; Virginia.

Keywords: Al/Si-ordering, sanidine megacrystals, optical anomalies

FA2-MS16-P24

Core-Shell Ni_{0.5}TiOPO₄/C Composites as Anode Materials in Li Ion Batteries. Rachid Essehli^a, Brahim ElBali^b, Zehn Zhou^c, Hartmut Fuess^d. ^a*SUBATECH, Unité Mixte de Recherche 6457, École des mines de Nantes, CNRS/IN2P3, Université de Nantes, BP 20722, 44307 Nantes cedex 3 France.* ^b*Laboratory of Mineral Solid and Analytical Chemistry "LMSAC", Department of Chemistry, Faculty of Sciences, University Mohamed I, PO Box 624, 60000 Oujda, Morocco.* ^c*Institute of New Energy Material Chemistry, Key Laboratory of Advanced Micro/Nanomaterials and Batteries/Cells (Ministry of Education), Nankai University, Tianjin*

300071, China. ^dMaterials Science, Technical University Darmstadt, Germany.
E-mail: essehli_rachid@yahoo.fr

Pure $\text{Ni}_{0.5}\text{TiOPO}_4$ was prepared via a traditional solid-state reaction, and then $\text{Ni}_{0.5}\text{TiOPO}_4/\text{C}$ composites with core-shell structure were synthesized by hydrothermally treating $\text{Ni}_{0.5}\text{TiOPO}_4$ in glucose solution. X-ray diffraction patterns confirmed that $\text{Ni}_{0.5}\text{TiOPO}_4/\text{C}$ crystallized in the monoclinic $\text{P}2_1/\text{c}$ space group. The morphology and the microstructure were characterized by scanning electron microscopy and transmission electron microscopy. The small particles with irregular shapes were coated with uniform carbon film of ~ 3 nm in thickness. Raman spectroscopy also confirmed the presence of carbon in $\text{Ni}_{0.5}\text{TiOPO}_4/\text{C}$ composites. The electrochemical performances of $\text{Ni}_{0.5}\text{TiOPO}_4/\text{C}$ and $\text{Ni}_{0.5}\text{TiOPO}_4$ were compared through galvanostatic charge/discharge tests, cyclic voltammetry and electrochemical impedance spectroscopy. $\text{Ni}_{0.5}\text{TiOPO}_4/\text{C}$ composites exhibited improved electrochemical performances due to the existence of carbon shell. During the first discharge, the NTP/C electrode delivered a capacity of 530mAh/g Fig 1. This high capacity corresponds the intercalation of more than 3 mol lithium ions per $\text{Ni}_{0.5}\text{TiOPO}_4$; however, not all lithium atoms could be extracted during the subsequent charge [1]. The redox couples of $\text{Ti}^{4+}/\text{Ti}^{3+}$, $\text{Ti}^{3+}/\text{Ti}^{2+}$ and Ni^{2+}/Ni in NTP/C can involve the insertion of only 3 mol lithium atoms. Therefore, the excess capacity during the first discharge should attribute to the formation of SEI passivation layer

[1] R. Essehli, B.E. Bali, H. Ehrenberg, I. Svoboda, N. Bramnik, H. Fuess, Mater. Res. Bull. 44 (2009) 817.

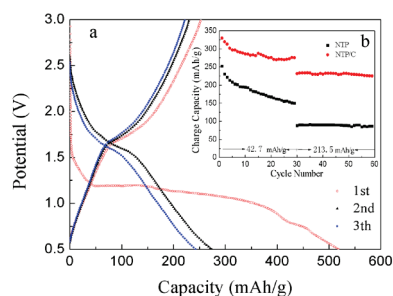


Fig. 1. The initial three galvanostatic charge/discharge curves of NTP (a) and the cycle performances of NTP and NTP/C measured at C/10 (42.7 mAh/g) and C/2 (213.5mAh/g) in the potential range of 0.5 to 3.0 V (b).

Keywords: $\text{Ni}_{0.5}\text{TiOPO}_4/\text{C}$, lithium-ion batteries, core-shell, anode materials

FA2-MS16-P25

X-ray diffraction study of σ -phase formation in super duplex stainless steel. Jorge Garin^a, Rodolfo Mannheim^a, Manuel Camus^b. ^aMetallurgical Engineering, Universidad de Santiago de Chile, Chile. ^bMechanical Engineering, Universidad de Antofagasta, Chile.

E-mail: jorge.garin@usach.cl

Super duplex stainless steels (SDSS) are two-phase alloys based on the iron-chromium system, with minor contents of molybdenum, nitrogen, tungsten and copper. Their remarkable mechanical and chemical properties make them suitable for

widespread industrial applications. The microstructure of these alloys is composed of approximately equal proportions of BCC ferrite and FCC austenite phases. However, exposure to elevated temperature processes causes embrittlement and loss of mechanical properties due to precipitation of intermediate phases, principally sigma-phase, in the microstructure. This phase is a complex intermetallic compound of Fe and Cr, based upon an ideal stoichiometric composition AX_2 , Pearson's code tP30 and space group $\text{P}4_2/\text{mmn}$, [1]. The formation of sigma-phase in cast ASTM A890 steel was investigated by means of quantitative X-ray diffraction. Three different temperatures (1023 K, 1073 K and 1123 K) and various annealing times (1 to 96 hours) were utilized in the experimental procedure. Owing to the usually complex powder diffraction pattern of the sigma compound, Rietveld refinements were performed based upon typical measurement and global parameters. The results obtained of the present study have assessed the application of the Rietveld method to quantify the formation of sigma-phase in SDSS subjected to annealing at relatively high temperatures. The refinement yielded the lowest R-values and much better represented the relative amount of phases in the samples. From the metallurgical standpoint, the results of XRD followed by Rietveld analysis indicated that the larger the annealing time of the alloy at a given temperature, the larger will be the volume fraction of the precipitated particles of sigma. Furthermore, sigma particles nucleates and grow reaching saturation levels depending on the specific type of the alloy.

[1] Yakel, H.L., *Acta Crystallogr.*, 1983, B39, 20.

Keywords: σ -phase, X-ray diffraction, duplex steels

FA2-MS16-P26

Microstructure of coke deposited by a high temperature process. Sven Gerhardt^a, Reiner Staudt^b, Klaus Bente^a, Jörg Hofmann^b. ^aInstitut für Mineralogie, Kristallographie und Materialwissenschaft, University of Leipzig. ^bInstitut für Nichtklassische Chemie, University of Leipzig.

E-mail: sven_gerhardt@uni-leipzig.de

It is well known that metal dusting is an undesirable corrosion phenomenon that can be observed in a wide range of chemically and petrochemically working industries. Due to strongly carburizing atmospheres, it leads to a decomposition of materials into metal particles and carbon. The aim of this work is to clarify open questions by identifying and modeling fundamental correlations between vapour-solid reactions and their consequences for microstructure, surface morphology and catalytic behaviour of the metal. The high temperature grown coke coating and metal pipe were inspected by 3D X-ray tomography (volume properties), XRD (existing phases), XPS (chemical bonding), HRTEM (nanostructures), SEM (surface morphology), electron microprobe analysis and TEM-EDX (chemical composition).

Keywords: transmission electron microscopy, X-Ray tomography, coke

FA2-MS16-P27

Mullite-type $(\text{Bi}_{1-x}\text{Sr}_x)_2\text{Al}_4\text{O}_{9-x/2}$: HT-XRPD, TEM and XPS investigations. Thorsten M. Gesing^a, Marco Schowalter^b, Claudia Weidenthaler^c, Andreas